Supporting Information

Template-assisted synthesis of novel $NiCoO_2$ nanocages/reduced graphene oxide composites as high-performance electrodes for supercapacitors

Xiao-Hui Guan,[a] Mu Li,[a] Hai-Zhen Zhang,[a] Liu Yang,[a] and Guang-Sheng Wang[b]*

[a]*School of Chemical Engineering, Northeast Electric Power University, Jilin 132000, P. R. China.*

[b]*Key Laboratory of Bio-Inspired Smart Interfacial Science and Technology of Ministry of Education, School of Chemistry and Environment, Beihang University, Beijing 100191, PR China.*

Synthesis of graphene oxides. In a typical procedure, pristine graphite powers (3 g, 325 mesh) was put into an 80 °C solution of concentrated H_2SO_4 (15 ml), $K_2S_2O_8$ (2.5 g), and P_2O_5 (2.5 g). The mixture was kept at 80 °C for 6h. Then, the mixture was diluted with 500 ml of de-ionized (DI) water. Then, the mixture was filtered and washed with water to remove the residual acid. The product was dried at 60 °C overnight to obtain pre-oxidized graphite powder. This powder was added into cold (0 °C) concentrated H_2SO_4 (115 ml). Then, $KMnO_4$ (15 g) was slowly added, with the temperature of mixture kept below 20 °C. After the addition of 250 ml of water (keep the temperature below 50 °C), the mixture was stirred for 2 h, and then an additional 700 ml of water was added. After that, 10 ml of 30% H_2O_2 was added into the mixture, and the solution changed into brilliant yellow, accompanied by the generation of bubbles. The mixture was filtered and washed with diluted HCl aqueous solution (10 wt.%, 1 L) to remove metal ions. The brownish yellow solution was centrifuged at 10,000 rpm, supernatant solution was decanted away, and the resulting material was subjected tomultiple washings with water until the pH was 7.

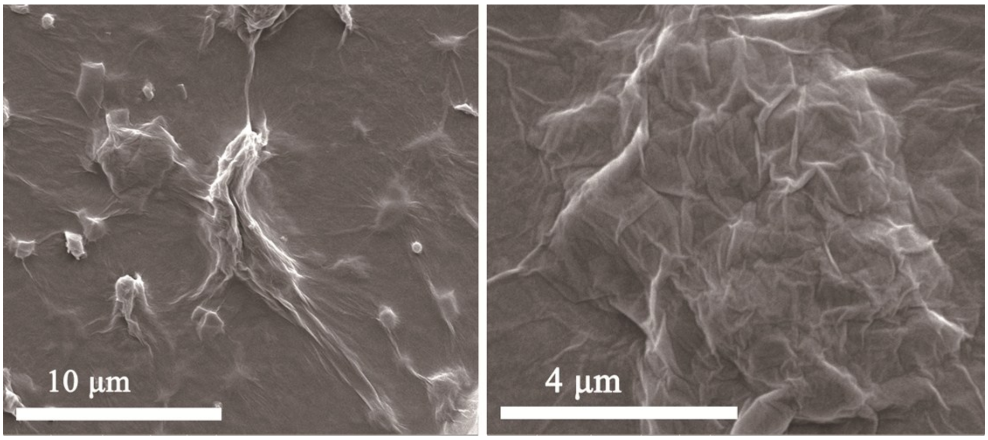

Fig. S1 SEM images of the GO

The surface morphologies of as synthesized GO were investigated by SEM as shown in typical SEM images with different magnifications (Fig. S1). It can be observed that GO have layered structure, which contains thin, wrinkled and folded region on its surfaces.

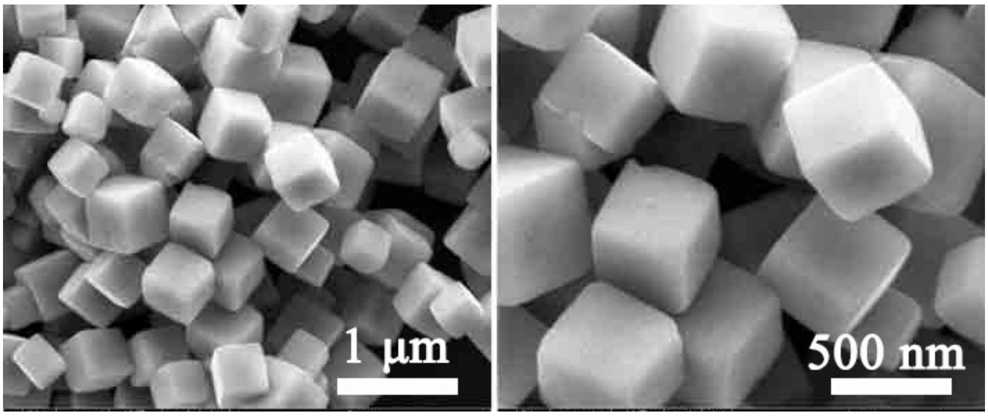

Fig. S2 SEM images of the as-prepared cubic Cu_2O.

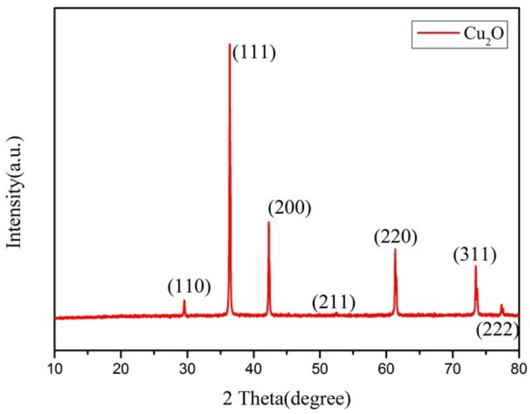

Fig. S3 XRD pattern of the as-prepared cubic Cu_2O

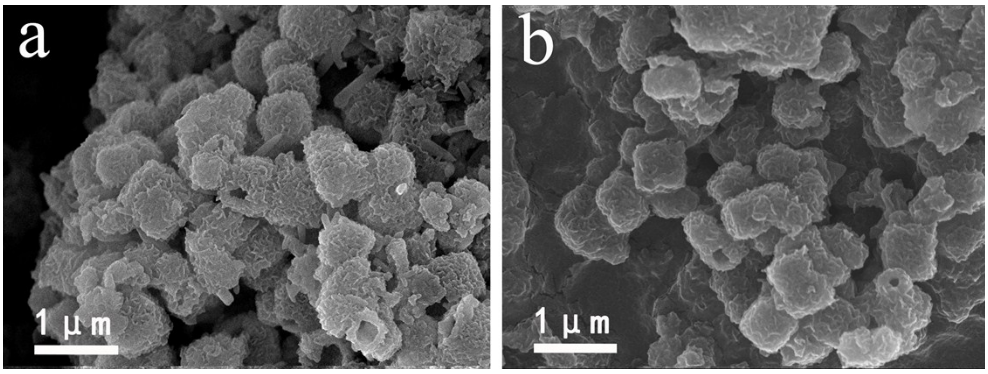

Fig. S4 SEM images of the as-prepared NiCo(OH)$_2$ and 1%NiCo(OH)$_2$/rGO: (A) NiCo(OH)$_2$; (B) 1%NiCo(OH)$_2$/rGO.

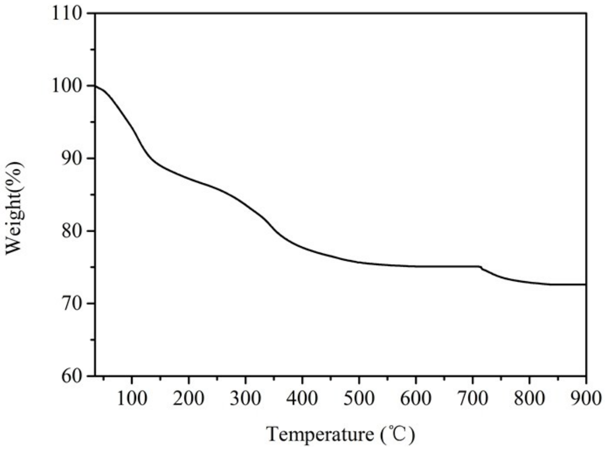

Fig. S5 TG pattern of NiCo(OH)$_2$/rGO in N$_2$ from 35 °C to 900 °C with a heating rate of 10 °C·min^{-1}.

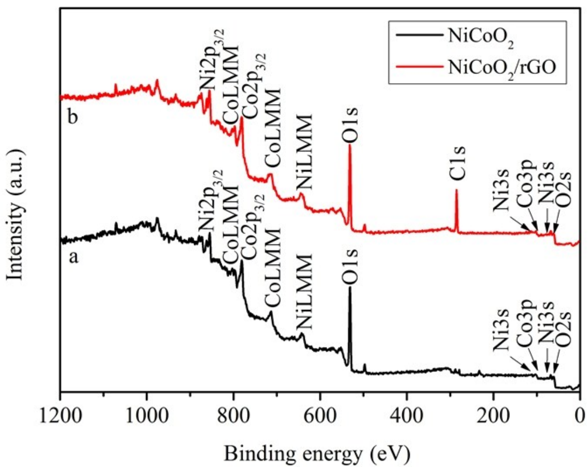

Fig. S6 XPS sunvery spectrum of the as-prepared NiCoO$_2$ and NiCoO$_2$/rGO.

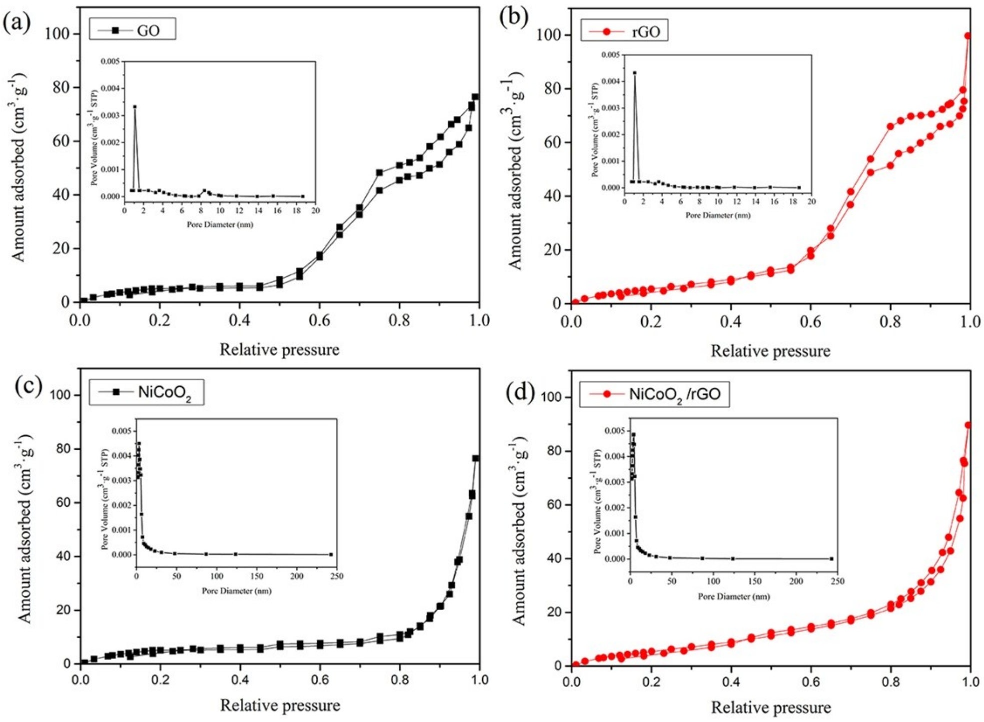

Fig. S7 N_2 adsorption-desorption isotherms of the GO, rGO, $NiCoO_2$, and 1% $NiCoO_2$/rGO

Table 1 Specific surface area of the samples

Sample	S_{BET} ($m^2 \cdot g^{-1}$)
GO	30.13
rGO	92.40
$NiCoO_2$	15.45
1% $NiCoO_2$/rGO	63.91

It can be seen in Figure S7 that the absorption of 1%$NiCoO_2$/rGO was higher than $NiCoO_2$ at high relative pressure range (1.0). It also indicates that 1% $NiCoO_2$/rGO processes a much higher BET surface area than $NiCoO_2$. The Brunauer-Emmett-Teller (BET) of the GO, rGO, $NiCoO_2$, and 1% $NiCoO_2$/rGO are 30.13, 92.40, 15.45 and 63.91 $m^2 \cdot g^{-1}$, shown in Table 1 respectively. It can be seen from Table 1 that the specific surface area of GO is much smaller than that of rGO. This may be because the layers of GO contain a large number of oxygen-containing groups. These groups are intertwined with each other, so their specific surface area is small; and after Na_2SO_3 reduction, The resulting rGO, because most of the oxygen-containing groups between the carbon layers are reduced and removed, the specific surface area increases, but it is still much smaller than the specific surface area of the single layer rGO (2630 $m^2 \cdot g^{-1}$), indicating that the obtained rGO is not ideal the single-layer rGO. After loading $NiCoO_2$, the specific surface area of rGO has decreased, which may be due to a portion of dispersed $NiCoO_2$ plugged rGO channel.

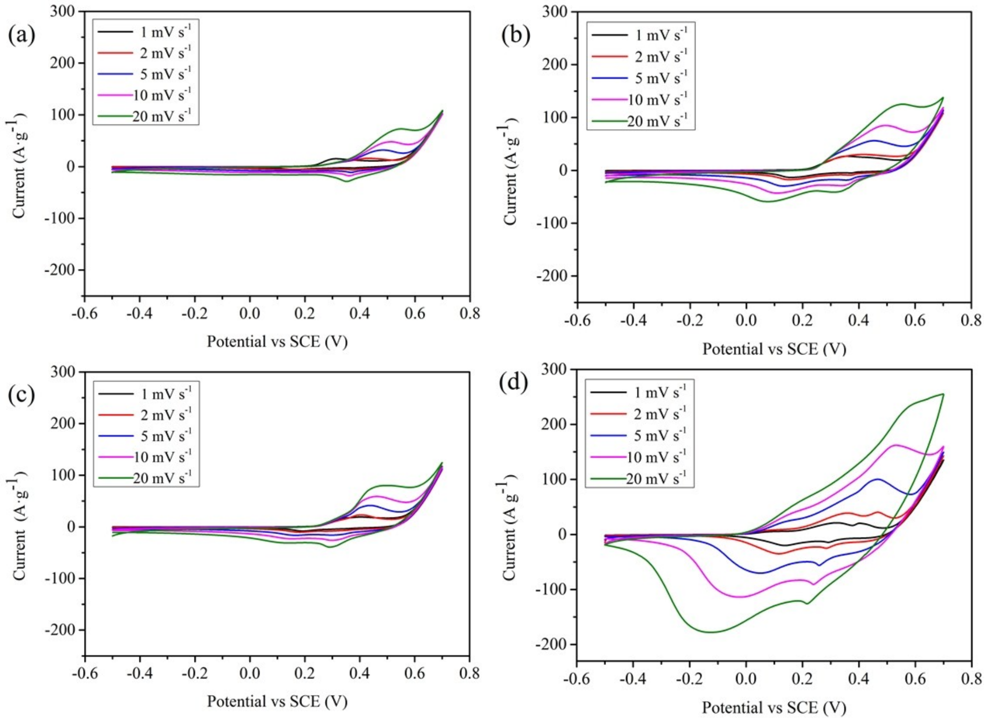

Fig. S8 CV curves of the electrodes at different scan rates: (A) $NiCo(OH)_2$; (B) $NiCo(OH)_2$/rGO; (C) $NiCoO_2$; (D) $NiCoO_2$/rGO

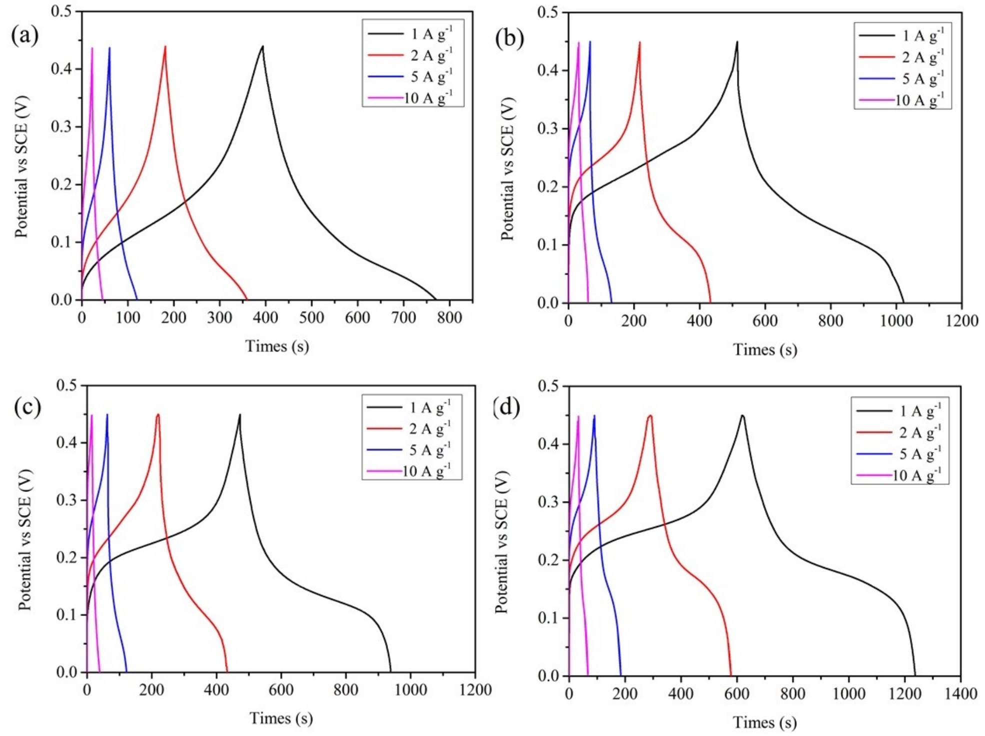

Fig. S9 GCD curves of the electrodes at various current densities: (A) $NiCo(OH)_2$; (B) $NiCo(OH)_2$/rGO; (C) $NiCoO_2$; (D) $NiCoO_2$/rGO

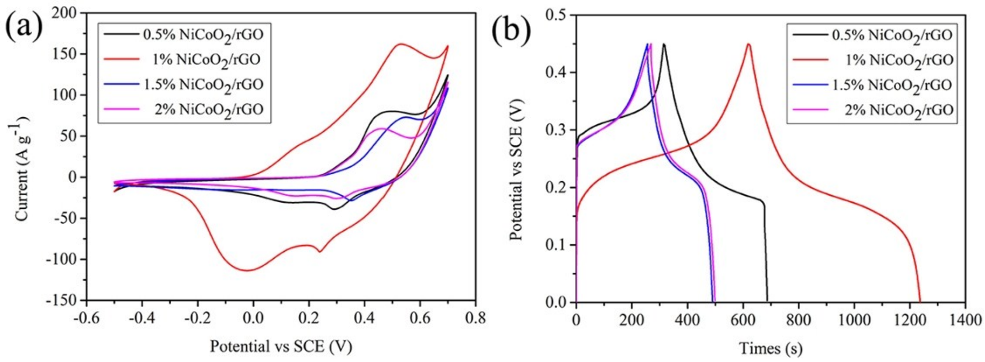

Fig. S10 CV and GCD curves of $NiCoO_2$/rGO composites with different weight ratios of rGO.

Table S2 Performance comparisons with other works

Materials	Morphology and structure	Current density	Specific capacitance	Capacitance after cycling	Reference
$NiCoO_2$	nanosheets	1 $A \cdot g^{-1}$	830 $F \cdot g^{-1}$	622 $F \cdot g^{-1}$ (2000cycles)	S1
$NiCoO_2$/rGO	nanoparticles	2 $A \cdot g^{-1}$	288 $F \cdot g^{-1}$	253 $F \cdot g^{-1}$ (1000cycles)	S2
$NiCoO_2$/rGO/$NiCoO_2$	sandwich nanosheets	1 $A \cdot g^{-1}$	784 $F \cdot g^{-1}$	686 $F \cdot g^{-1}$ (2000cycles)	S3
NRGO–$NiCoO_2$	nanoflakes	2 $A \cdot g^{-1}$	386 $F \cdot g^{-1}$	358 $F \cdot g^{-1}$ (2000cycles)	S4
Co_9S_8	multilayered plates	1 $A \cdot g^{-1}$	788 $F \cdot g^{-1}$	448 $F \cdot g^{-1}$ (10000cycles)	S5
Co_3O_4	nanosheet	1 $A \cdot g^{-1}$	495 $F \cdot g^{-1}$	470 $F \cdot g^{-1}$ (1000cycles)	S6
NiO	nanoflakes	2 $A \cdot g^{-1}$	381 $F \cdot g^{-1}$	339 $F \cdot g^{-1}$ (1000cycles)	S7
C@$NiMoO_4$	nanograins	1 $A \cdot g^{-1}$	269 $F \cdot g^{-1}$	237 $F \cdot g^{-1}$ (1000cycles)	S8
$NiCoO_2$/rGO	nanocages	1 A/g	1375 F/g	778 F/g (3000cycles)	This work

References

[S1] S. Jiang, Y Sun, Z. Li, et al. *Journal of the Electrochemical Society*, 2017, 164(6), A1158-A1164.

[S2] H. Z. WANG, L. Yu, et al. *Chemical Research in Chinese Universities*, 2017, 33(4), 1-5.

[S3] X. Leng, Y Shao, L Wu, et al. *Journal of Materials Chemistry A*, 2016, 4(26).

[S4] Y. Chen, Y. Xu, J. Wei, et al. *Journal of Materials Chemistry A*, 2015, 3(13), 7121-7131.

[S5] T. Yao, Y. Li, D. Liu, et al. *Journal of Power Sources*, 2018, 379: 167-173.

[S6] N. Yu, Q. Huang, N. Fu, et al. *Rsc Advances*, 2016.

[S7] J. Zhao, H. Liu, Q. Zhang. *Applied Surface Science*, 2017, 392:1097-1106.

[S8] C. Wei, Y. Huang, J. Yan, X. F. Chen, X. Zhang, *Ceram. Int*. 2016, 42, 15694-15700.